

EVIDENCE FOR A NEW SCALAR MESON

N.M. Cason
University of Notre Dame*
Notre Dame, Indiana 46556



Abstract: We have observed the production of a new scalar meson in the reaction $\pi^- p \rightarrow n K_s^0 K_s^0$ at 6 and 7 GeV/c. The meson has a mass and width of 1255 MeV and 80 MeV respectively. The meson is observed primarily through the interference of the S-wave and D-wave $K_s^0 K_s^0$ production amplitudes. Both the S-wave amplitude and phase are observed to have resonance-like behavior. The quantum numbers preferred for the meson are $J^P = 0^+$ and $C = +1$.

Résumé: Nous avons observé la production d'un nouveau meson scalaire dans la réaction $\pi^- p \rightarrow n K_s^0 K_s^0$ à 6 et 7 GeV/c. Le meson présente une masse et une largeur de 1255 MeV et 80 MeV respectivement. Le meson est observé surtout à travers l'interférence des ondes S et D des amplitudes de production pour $K_s^0 K_s^0$. On a observé que l'amplitude de l'onde-S et sa phase présentent tout les deux un comportement de résonance. Les numéros quantiques préférés par le meson sont $J^P = 0^+$ et $C = +1$.

*Research supported in part by the National Science Foundation.

*Recherche soutenu part la National Science Foundation.

We report the results of an analysis of an experiment carried out at the Argonne National Laboratory ZGS utilizing the 1.5 m streamer-chamber facility. The experiment was designed to study the reaction



The experimental configuration is shown in Fig. 1. Briefly, the trigger required an incident beam particle into the liquid hydrogen target in the streamer chamber, no charged particle emerging from the target, and at least two counters in a hodoscope downstream of the streamer chamber to fire. Some 400,000 pictures were taken, approximately 70% at 7 GeV/c and the remainder at 6 GeV/c.

The data were scanned, measured and then processed by TVGP and SQUAW. About 8% of the 400,000 events were "double-vee" topologies and were measured; and some 16,000 events resulted as candidates for the $K_s^0 K_s^0$ production. Figure 2 shows the effective-mass distribution

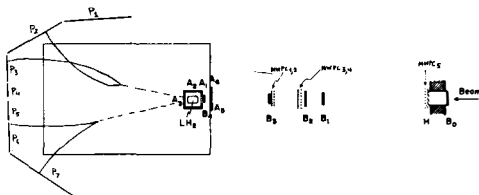


Figure 1

Elevation view of the experimental configuration (not to scale). The B counters are beam-defining scintillation counters. The P

counters are a scintillation hodoscope detecting charged particle decays of the neutral strange particles. The beam momentum is tagged by the scintillation hodoscope H and a multi-wire proportional chamber (MWPC). MWPC's are also used to measure the incident angles of the beam track. The A counters are anti-counters.

tion for the decay tracks from which we estimate $\sigma \approx 10$ MeV. Figure 3 shows the missing-mass-squared distribution for events consistent with $K_s^0 K_s^0$ production. The neutron peak is very prominent with very little background under it. After appropriate χ^2 cuts and fiducial volume cuts, we obtain a final sample of 5096 unweighted events corresponding to reaction (1). These events were then weighted using a Monte Carlo technique.

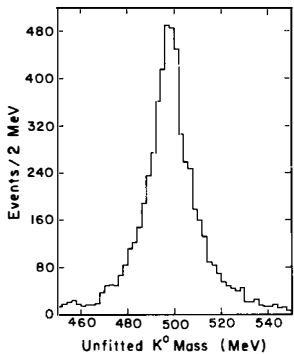
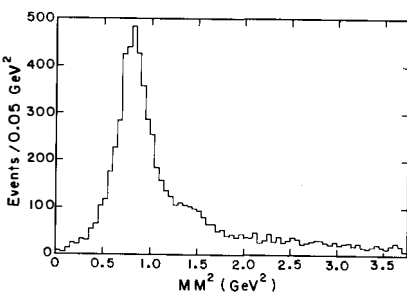


Figure 2

Measured effective-mass distribution of the K decay tracks.

Figure 3

Missing-mass-squared distribution for events for which both neutral particles are K_s^0 's.



The effect of the weighting is shown in Figs. 4, 5, 6 and 7. These show the effective mass distribution, t -distribution, $\cos \theta_J$ distribution vs $M(K_s^0 K_s^0)$; and ϕ_{TY} distribution vs $M(K_s^0 K_s^0)$. In each case both the unweighted and weighted distributions are shown. From these one can see that our weights are very uniform, very slowly varying, and are nowhere extremely small. This results in part from the high energy of the experiment and in part from the very large solid angle subtended by the charged-

particle hodo-

scope. This

feature is the

primary advan-

tage the

Fig. 4

Weighted and unweighted (shaded) $K_s K_s$ effective-mass distribution for the final data sample.

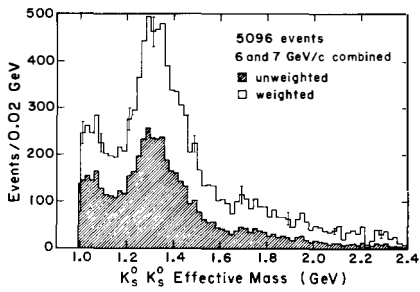
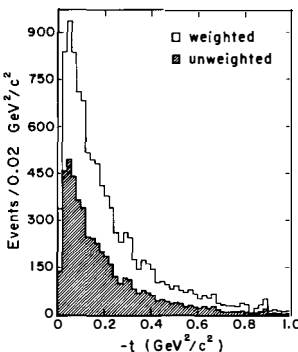


Figure 5

Weighted and unweighted (shaded) t distribution for the final data sample.



present experiment has with respect to earlier experiments.

Figure 6

Weighted and unweighted (shaded) distributions of $\cos \theta_J$ for various $K_s^0 K_s^0$ effective mass ranges.

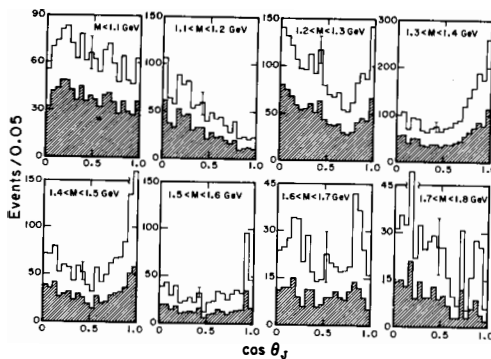
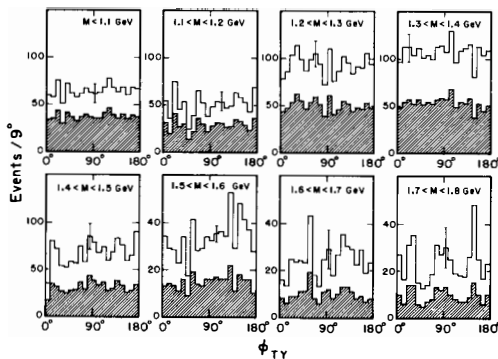


Figure 7

Weighted and unweighted (shaded) distributions of ϕ for various $K_s^0 K_s^0$ effective mass ranges.



In Fig. 8 is shown the $K_s^0 K_s^0$ effective mass distribution for various t -ranges. Here we note that the low mass S^* peak is quite apparent for $t < 0.2 (\text{GeV}/c)^2$ and is not clearly present for higher t . We also note that the shape of the broad enhancement from 1250 to 1450 MeV seems to be very strongly t -dependent. The peak seen for $t > 0.5 (\text{GeV}/c)^2$ is consistent with A_2^0 production on a rather flat background, whereas the

the peak at low t has a much broader character. It is this broad bump which has been the subject of much discussion in the past¹⁻⁵ and which we will study in detail here.

Figure 8
Weighted $K_s^0 K_s^0$ effective-mass distribution for various ranges of t .

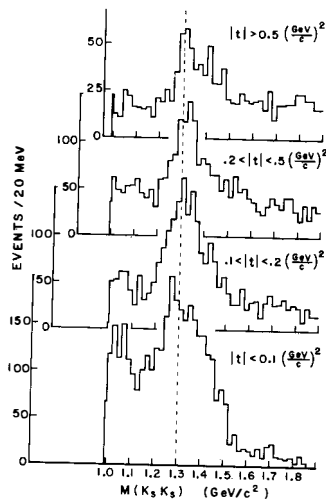


Figure 9 shows the unnormalized moments $\sqrt{4\pi} N \langle Y_\ell^m \rangle$, as a function of $M(K_s K_s)$. (We have found that moments with $\ell > 4$ and $m > 2$ are consistent with zero.) The most notable behavior is in the Y_2^0 and Y_4^0 moments. The Y_2^0 moment primarily represents S - D interference and the Y_4^0 moment, the D wave intensity. It is clear that the S - D wave interference is strong and is varying rapidly (but smoothly). The $m \neq 0$ moments are typically near zero as would be expected from a simple one-pion-exchange production process at low t . An analysis³ by the EMS group at Argonne has shown good evidence for $f - f'$ interference in the reaction $\pi^- p \rightarrow n K^+ K^-$. Our data are consistent with this hypothesis and require a broad f' if no other effects are present. Our

best fit has $\Gamma(f')$ \sim 80 MeV and a ratio of f' to f production (for $|t| < .2$ $(\text{GeV}/c)^2$) of 0.14.

Figure 9

Unnormalized moments $\langle Y_\ell^m \rangle$ as a function of M_{KK} for $|t| < 0.2$ GeV^2 .

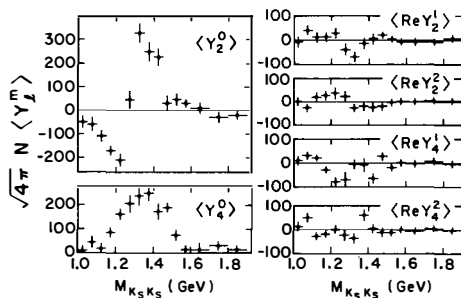


Figure 10 shows the dependence of the S wave amplitude, the amplitudes D_0 , D_{1+} and D_{1-} , and $|\phi_S - \phi_D|$ the S-wave - D-wave phase difference as a function of $M(K_S^0 K_S^0)$. Here we have used the relations:

$$(4\pi)^{1/2} N \langle Y_0^0 \rangle = S^2 + D_0^2 + D_{1+}^2 + D_{1-}^2$$

$$(4\pi)^{1/2} N \langle Y_2^0 \rangle = 2SD_0 \cos \phi_{SD} + (2\sqrt{5}/7)D_0^2 + \sqrt{5}/7(D_{1+}^2 + D_{1-}^2)$$

$$(4\pi)^{1/2} N \langle \text{Re} Y_2^1 \rangle = -\sqrt{2}SD_{1-} \cos \phi_{SD} - \sqrt{10}/7D_0D_{1-}$$

$$(4\pi)^{1/2} N \langle \text{Re} Y_2^2 \rangle = -\sqrt{30}/14(D_{1+}^2 - D_{1-}^2)$$

$$(4\pi)^{1/2} N \langle Y_4^0 \rangle = 6/7D_0^2 - 4/7(D_{1+}^2 + D_{1-}^2)$$

$$(4\pi)^{1/2} N \langle \text{Re} Y_4^1 \rangle = -\sqrt{60}/7D_0D_{1-}$$

$$(4\pi)^{1/2} N \langle \text{Re} Y_4^2 \rangle = \sqrt{10}/7(D_{1+}^2 - D_{1-}^2)$$

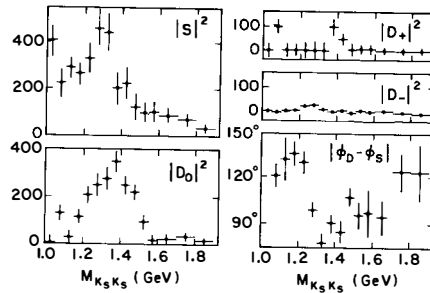
(D_{1+} and D_{1-} are the natural and unnatural parity exchange linear combinations of D_1 and D_{-1} amplitudes.) The validity of these

relations is based on the following assumptions:

- 1) $D_{2+} = D_{2-} = \text{zero}$ (consistent with $Y_{\ell}^m = 0$ if $m > 2$).
- 2) No G-waves or higher are present (consistent with $Y_{\ell}^m = 0$ if $\ell > 2$).
- and 3) Phase coherence (i. e. all D-wave phases are the same).

Figure 10

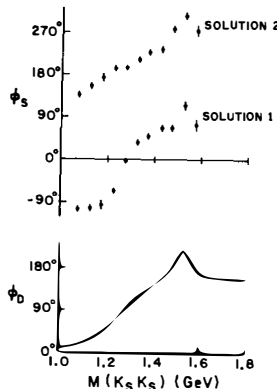
S- and D-wave intensities and the S - D wave phase difference resulting from the amplitude analysis described in the text.



We note that the data require a large S-wave intensity in the 1300 MeV region. In order to see if the peak in S-wave intensity corresponds to a resonance amplitude, we have determined the S-wave phase as a function of energy. Since the variable determined by the data is $|\phi_S - \phi_D|$ we have assumed a phase variation of the D-wave to be given by the $f - f'$ fit to the Y_4^0 moment discussed above. The S and D wave phases are shown in Fig. 11. We note that there are two solutions to the S-wave phase because of the ambiguities introduced by the fact that only the magnitude of the S-wave - D-wave phase is determined by the data. Note also that the D-wave phase is primarily due to the $f -$ Breit-Wigner below 1450 MeV and not strongly influenced by the $f - f'$ interference hypothesis.

Figure 11

a) The D-wave phase using the f^0 Breit-Wigner as modified by $f-f'$ interference.
 b) The S-wave phase resulting from combining (a) with the $|\phi_S - \phi_D|$ result from the amplitude analysis. Both solutions are shown.



The two S-wave solutions in Fig. 11 both show significant phase variation with energy. Solution 1 is indicative of a rapid variation as the energy passes through 1255 MeV, near the peak in the mass distribution and is the likely correct solution if the S-wave is indeed resonant. The phase variation indicates a width of $\Gamma \sim 80$ MeV.

We conclude from the intensity and phase variation of the S-wave amplitude that we have observed a new S-wave resonance at ~ 1255 MeV. It clearly has $J^P = 0^+$. From this it also follows that $G = +1$. The $K_S K_S$ decay mode independently requires $C = 1^+$ for the resonance. Further work is being carried out to determine the i-spin of the resonance.

References

1. W. Beusch et al., Physics Letters 25B, 357 (1967).
2. T. F. Hoang et al., Phys. Rev. Letters 21, 316 (1968).
3. A.J. Pawlicki et al., Argonne preprint ANL-HEP-CP-75-50, (1975).
4. A.J. Pawlicki et al., Argonne preprint ANL-HEP-75-09, (1975).
5. W. Beusch et al., CERN preprint (submitted to Phys. Letters) (1975).